Reexamination of the variational Bose-Hubbard model

Jan Major,[1] Mateusz Łącki,[1] and Jakub Zakrzewski[1,2]
[1]*Institute of Physics, Jagiellonian University, ulica Reymonta 4, 30-059 Kraków, Poland*
[2]*Mark Kac Complex Systems Research Center, Jagiellonian University, ulica Reymonta 4, 30-059 Kraków, Poland*
(Received 11 December 2013; published 30 April 2014)

For strongly interacting bosons in optical lattices, the standard description using the Bose-Hubbard model becomes questionable. The role of excited bands becomes important. In such a situation, we compare results of simulations using the multiband Bose-Hubbard model with a recent proposition based on a time-dependent variational approach. It is shown that the latter, in its original formulation, uses a too small variational space, often leading to spurious effects. Possible expansion of the variational approach is discussed.

DOI: 10.1103/PhysRevA.89.043626 PACS number(s): 67.85.Hj, 03.75.Kk, 03.75.Gg, 03.65.Ud

I. INTRODUCTION

Ultracold bosonic atoms in an optical lattice potential have been a very active field of both experimental and theoretical research. They enable one to prepare and study a broad spectrum of complex quantum systems in well-controlled experiments. Of particular importance is experimental research, using ultracold quantum gases, of systems which mimic various condensed-matter Hamiltonians. For a complete review, please see Refs. [1,2]. The key stimulus for these activities is the existence of the mapping from a continuous model [3], describing a gas of ultracold atoms in an optical lattice potential [4] to a discrete Bose-Hubbard (BH) model.

By choosing a proper setup of lasers forming an optical lattice, various lattice geometries and dimensionalities may be realized [5,6]. In particular, one may obtain a one-dimensional lattice [7], which is then mapped to a one-dimensional Bose-Hubbard model. One dimension makes interactions and correlations relatively strong [8,9] driving the system far from the mean-field regime [10]. The mapping is performed by expanding the field operator in localized modes with the help of Wannier functions [11,12]. Although often, restriction to the lowest Bloch band, leading to a standard Bose-Hubbard model [4] is sufficient, for stronger interactions, higher bands become significant as already realized quite early [13–15]. Near a Feshbash resonance, for a large scattering length, an optical lattice may strongly modify atom-atom interactions [14,16–21], making a lowest band description of the problem questionable too.

Taking higher bands into account leads to a numerically challenging problem as it exponentially increases the on-site Hilbert-space dimension with the number of bands. It hampers further any direct diagonalization of the problem. Even the application of the very successful density-matrix renormalization-group method [22] in the multiband case is questionable as its time complexity also increases very fast with the on-site Hilbert-space dimension limiting any serious computation for bosons to, at most, two to four bands.

In recent years, another approach to the strongly interacting bosons in a lattice has been proposed [23–27]. The higher bands are included in the local single-site Hamiltonian. Its diagonalization yields ground states corresponding to different numbers of particles at a site; this new basis is then used instead of the usual Fock basis to reexpress the Hamiltonian. In effect, instead of a multiband Hamiltonian, one obtains an effective single-band model with occupation-dependent parameters. Evaluation of them is quite costly, numerically due to a large dimension of the local Hilbert space describing a configuration of particles within one lattice site. Additionally, convergence problems may arise, and the theory may fail to represent the physical system for strong interactions in part due to a neglect of long-range tunneling of particles in highly excited bands. In effect, the efficient description of strongly interacting atoms in optical lattices, even for the simplest contact interactions, remains an unsolved problem.

Recently, a new, different in spirit and potentially efficient, proposal for an approximation, designed to address the convergence as well as the large Hilbert-space dimension problems, has been performed [28]. Authors use a time-dependent variational (TDV) principle to optimize a single one-particle Wannier function per site. Its shape also is altered by interactions with the other particles during the evolution, whereas, in the standard approach [29], Wannier functions depend solely on the instantaneous strength of the optical lattice potential, i.e., on a single-particle physics. In the variational approach, a dynamic change in the Wannier functions may be a substantial improvement by allowing them to be optimally chosen. The proposed approach seems quite promising, and the question remains if and under what assumptions this method provides an alternative approach for the treatment of realistic problems. This is the problem we want to address in this paper.

We discuss the multiband BH (MBH) model reduced to one dimension in Sec. II, whereas, Sec. III offers necessary information concerning the time-dependent variational approach. Comparison of both approaches is given in Sec. IV, both on the ground-state and on the different time-dependent dynamical problems. We restrict ourselves to small model systems that, nevertheless, allow us to compare both methods. A simple generalization of the variational approach and its possible advantages is discussed in Sec. V with the subsequent section presenting our conclusions.

II. THE MULTIBAND BOSE-HUBBARD MODEL

The ultracold interacting gas of bosons in the optical lattice potential is described by a second quantized Hamiltonian,

$$\hat{H} = \int d^3r\, \Psi^\dagger(\vec{r})\hat{h}(\vec{r})\Psi(\vec{r}) + \frac{1}{2}\int d^3r\, d^3r' \Psi^\dagger(\vec{r})\Psi^\dagger(\vec{r}')V(\vec{r},\vec{r}')\Psi(\vec{r})\Psi(\vec{r}'), \quad (1)$$

where $\hat{h} = -\frac{\hbar^2}{2m}\nabla^2 + V_{\rm lat}(\vec{r})$ is a one-particle Hamiltonian and

$$V(\vec{r},\vec{r}') = \frac{4\pi\hbar^2 a}{m}\delta^{(3)}(\vec{r}-\vec{r}') = g\delta^{(3)}(\vec{r}-\vec{r}') \tag{2}$$

is a contact pseudopotential modeling the s-wave scattering interaction with a being the scattering length. Formally, to avoid problems with the Hermiticity of the above Hamiltonian [30], instead of the Dirac-δ interaction, one should use a pseudopotential of the form

$$V(\vec{r},\vec{r}') = g\delta(\vec{r}-\vec{r}')\frac{\partial}{\partial|\vec{r}-\vec{r}'|}|\vec{r}-\vec{r}'|. \tag{3}$$

However, in the multiband expansion, one typically uses a basis spanned by smooth Wannier functions truncated to the first few Bloch bands (for details, see the next section). In that case, the potential (3) is equivalent to the simplified Dirac-δ potential (2).

In the following, we consider a quasi-one-dimensional geometry assuming $V_{\rm lat}(\vec{r}) = s\,\sin^2(kx) + \frac{1}{2}m\Omega^2(y^2+z^2)$, where Ω is a frequency of a tight transverse harmonic trapping potential. In these transverse directions, we assume that only the ground-state mode ϕ_0 is occupied. For a given lattice depth s, the field operator is expanded as

$$\Psi(\vec{r}) = \sum_{i,\alpha} a_i^\alpha W_i^\alpha(\vec{r}), \tag{4}$$

with

$$W_i^\alpha(\vec{r}) = w_i^\alpha(x)\phi_0(y)\phi_0(z), \tag{5}$$

where $w_i^\alpha(x)$ is the standard (assumed real) one-dimensional Wannier function of the α band [11] localized at site i. Performing integrations in Eq. (1), the multiband model is obtained

$$\hat{H} = -\sum_{i\neq j,\alpha} J_{i-j}^\alpha\left(\hat{b}_i^{\alpha\dagger}\hat{b}_j^\alpha + \text{H.c.}\right) + \sum_{i,\alpha} E_i^\alpha \hat{n}_i^\alpha + \frac{1}{2}\sum_{\alpha,\beta,\gamma,\delta}\sum_{ijkl} U_{ijkl}^{\alpha\beta\gamma\delta}\hat{b}_i^{\alpha\dagger}\hat{b}_j^{\beta\dagger}\hat{b}_k^\gamma\hat{b}_l^\delta. \tag{6}$$

The tunneling from site j to i (along the x direction) in the α band is

$$J_{i-j}^\alpha = \int w_i^\alpha(x)\left[-\frac{\hbar^2}{2m}\frac{d^2}{dx^2} + s\,\sin^2(kx)\right]w_j^\alpha(x)dx, \tag{7}$$

with mean energies at the sites in different bands $E_i^\alpha = J_0$ being independent of the site. Often in experiments, an additional slowly varying harmonic trap potential is present, which may be taken into account in E_i^α's. For the purpose of the present paper, such terms are not relevant and are dropped for simplicity. The interaction integrals read

$$U_{ijkl}^{\alpha\beta\gamma\delta} = g\int dx\, w_i^\alpha(x)w_j^\beta(x)w_k^\gamma(x)w_l^\delta(x), \tag{8}$$

with

$$g = \frac{4\pi\hbar^2 a}{m}\int dy\,dz|\phi_0(y)|^4|\phi_0(z)|^4 \tag{9}$$

being a modified contact interaction strength due to a reduction of the problem to one dimension. In terms of the transverse trap frequency, it reads $g = 2\hbar a\Omega$.

For sufficiently deep lattices (with depth s of a few energy recoils $E_R = \hbar^2k^2/2m$), one may perform a standard approximation neglecting long-range tunnelings J_{i-j} for $|i-j| \geqslant 2$ and keeping nearest-neighbor tunnelings J_1 only (later, we drop the subscript and denote this tunneling simply as J following a standard convention). Similarly, often only the on-site interactions terms $U_{ijkl}^{\alpha\beta\gamma\delta}$ for $(i,j,k,l) = (i,i,i,i)$ are taken into account since other integrals are significantly smaller. Recently however, it has been stressed [24,26,27,31] that contributions $U_{ijkl}^{\alpha\beta\gamma\delta}$ for $(i,j,k,l) = (i,i,i,j)$ (up to a permutation) may not be easily dismissed. They have a character of density-dependent tunnelings, and they may compete with standard tunnelings (especially for deep lattices, strong interactions, or high density), leading to significant measurable effects.

Although we could take these terms into account, we choose to neglect them in the following to concentrate on the comparison between the multiband and the variational approach on a standard Bose-Hubbard system without density-dependent tunnelings as introduced in Ref. [28].

With these assumptions, the MBH Hamiltonian reads

$$\hat{H}_{\rm MBH} = \sum_{k=1}^{L}\left(-\sum_{\alpha=1}^{\mathcal{N}} J^\alpha\left(\hat{b}_k^{\alpha\dagger}\hat{b}_{k+1}^\alpha + \text{H.c.}\right) + \sum_{\alpha=1}^{\mathcal{N}} E_k^\alpha\hat{n}_k^\alpha + \frac{1}{2}\sum_{\alpha,\beta,\gamma,\delta}^{\mathcal{N}} U^{\alpha\beta\gamma\delta}\hat{b}_k^{\alpha\dagger}\hat{b}_k^{\beta\dagger}\hat{b}_k^\gamma\hat{b}_k^\delta\right), \tag{10}$$

where $\mathcal{N}$ is the number of bands taken and we have dropped the subscripts on interaction constants as they become, within the assumed model, independent of the sites. The above Hamiltonian is used in the simulations in the subsequent sections. It is also a basis for the formulation of the variational system of equations of motion described in the next section.

III. THE TIME-DEPENDENT BOSE-HUBBARD MODEL FROM THE VARIATIONAL PRINCIPLE

While forming a single-band BH model, a special case of the MBH, one neglects the contribution from higher Bloch bands. For strong interparticle interactions, this may significantly alter the results.

There have been attempts at restricting the Hamiltonian (10) to a relevant Hilbert subspace [23,24,26,27,31] by renormalizing the single-band BH model's parameters to density-dependent values including effective influence of the higher bands. This approach is suitable only for low-energy physics when excited bands are not populated.

Another interesting variational approach to simulate multiband effects has originally been proposed in Ref. [28]. We review its formulation below for self-containment of the paper. This variational single-band model assumes that particles do not populate single-particle modes defined by the ordinary Wannier functions but time-dependent modes formed by linear combinations of Wannier functions with appropriate time-dependent coefficients $d_k^\alpha(t)$. For one-dimensional systems,

this gives

$$w_k(x,t) = \sum_{\alpha=1}^{\mathcal{N}_V} d_k^\alpha(t) w_k^\alpha(x), \tag{11}$$

with $w_k^\alpha(x)$ being the standard (time-independent) Wannier functions also used in the previous section. The coefficients are allowed to vary in time and are chosen variationally by the TDV principle [32–35].

The novel idea in this approach is that the dynamics of Wannier functions $w_k(x,t)$ is set by the variational principle and not simply determined by, e.g., the time dependence of the optical lattice potential depth. By construction, they are mutually orthogonal and may be assumed to form the orthonormal set: $\langle w_i(t)|w_j(t)\rangle = \delta_{ij}$. Many boson wave functions are defined as

$$|\Psi(t)\rangle = \sum_{\vec{n}} C_{\vec{n}}(t)|\vec{n};t\rangle, \tag{12}$$

where $|\vec{n};t\rangle$ in the position representation is

$$|\vec{n};t\rangle = \frac{1}{\sqrt{n_1!\cdots n_L!}} \sum_{\pi\in S_N} w_{s(1)}(x_{\pi(1)},t)\cdots w_{s(N)}(x_{\pi(N)},t).$$

Here $s(n)$ is a sequence for which exactly n_l terms take a value of l. This construction defines a variational manifold embedded in the full Hilbert space of the problem. Observe that all the particles at a given site occupy the same time-dependent mode. Thus, by construction, they are in a separable state where multiparticle entanglement is absent.

State $|\vec{n};t\rangle$ depends on time via the time dependence of Wannier functions $w_i(\vec{x},t)$. Thus, creation and annihilation operators for bosons are also time dependent and are denoted by $\hat{b}_k(t)$ and $\hat{b}_k^\dagger(t)$. At any time t, a commutation relation $[\hat{b}_k(t),\hat{b}_q^\dagger(t)] = \delta_{kq}$ is fulfilled. In the complete analogy to the ordinary Bose-Hubbard Hamiltonian, one may define a time-dependent Bose-Hubbard model [28],

$$\hat{H}_V = \sum_{k=1}^{L}\Big[-J_{kk+1}(t)\hat{b}_k^\dagger(t)\hat{b}_{k+1}(t) + \text{H.c.} + E_k\hat{n}_k(t) + \frac{1}{2}U_{kkkk}(t)\hat{n}_k(t)[\hat{n}_k(t)-1]\Big], \tag{13}$$

where $J_{kk+1}(t)$, $E_k(t)$, and $U_{kkkk}(t)$ are the hopping integral, the on-site energy, and the interaction strength parameter defined, respectively, as

$$J_{kk+1}(t) = -\int w_k^*(x,t)\hat{h}(x)w_{k+1}(x,t)dx, \tag{14}$$

$$E_k(t) = \int w_k^*(x,t)\hat{h}(x)w_k(x,t)dx, \tag{15}$$

$$U_{kkkk}(t) = g\int w_k^*(x,t)w_k^*(x,t)w_k(x,t)w_k(x,t)dx. \tag{16}$$

A standard formulation of the TDV principle assumes a minimization of the action functional (Lagrange multipliers μ_i are added to preserve the orthonormality of the variational Wannier functions),

$$S(C_{\vec{n}},d_k^\alpha) = \int \langle\psi|\hat{H}_V - i\partial_t|\psi\rangle - \sum_i \mu_i(t)(\langle w_i(x,t)|w_i(x,t)\rangle - 1)dt. \tag{17}$$

Evolution equations for a vector $|\dot{w}_k(t)\rangle$ and Fock-space coefficients $C_{\vec{n}}$ follow:

$$i|\dot{w}_k(t)\rangle = \hat{P}_k(x,t)\Big[\sum_{l=k\pm1}^{M}\frac{\rho_{kl}(t)}{\rho_{kk}(t)}\hat{h}(x)|w_l(x,t)\rangle + \hat{h}(x)|w_k(x,t)\rangle + \frac{\rho_{kkkk}(t)}{\rho_{kk}(t)}U_{kk}(x,t)|w_k(x,t)\rangle\Big], \tag{18}$$

$$i\dot{C}_{\vec{n}}(t) = \sum_{\vec{n}'}\langle\vec{n}|\hat{H}_V(t)|\vec{n}'\rangle C_{\vec{n}'}(t), \tag{19}$$

where $\hat{P}_k(x,t)$ are projectionlike operators,

$$\hat{P}_k(x,t) = \sum_{\alpha=1}^{\mathcal{N}_V}\big|w_k^\alpha(x)\big\rangle\big\langle w_k^\alpha(x)\big| - |w_k(x,t)\rangle\langle w_k(x,t)|,$$

with

$$\rho_{kl} = \langle\psi(x,t)|\hat{b}_k^\dagger(t)\hat{b}_l(t)|\psi(x,t)\rangle,$$
$$\rho_{kkkk} = \langle\psi(x,t)|\hat{b}_k^\dagger(t)\hat{b}_k^\dagger(t)\hat{b}_k(t)\hat{b}_k(t)|\psi(x,t)\rangle$$

and $U_{kk}(x,t) = g|w_k(x,t)|^2$.

Explicitly working out all the terms of Eq. (18) that couple different components of a vector $d_k(t)$ yields

$$\dot{d}_k^a(t) = (\cdots) + i\sum_{\alpha,\beta,\gamma}^{\mathcal{N}_V} U_{kkkk}^{a\alpha\beta\gamma}(t)d_k^{\alpha*}(t)d_k^\beta(t)d_k^\gamma(t) - i\sum_{\alpha\beta\gamma\delta}^{\mathcal{N}_V} U_{kkkk}^{\alpha\beta\gamma\delta}(t)d_k^{\alpha*}(t)d_k^{\beta*}(t)d_k^\gamma(t)d_k^\delta(t)d_k^a(t). \tag{20}$$

The parity symmetry of the Wannier functions implies that $U_{kkkk}^{\alpha\beta\gamma\delta} \neq 0$ only if sum $\alpha+\beta+\gamma+\delta$ is even. If all d_k^α's for even (odd) α's are set initially to 0, then $\dot{d}_k^\alpha = 0$ for all t's.

IV. SIMULATIONS

The MBH model as an approximation of the true Hamiltonian (1) is not very practical. Even restricting the single-site space considering states with maximal occupation of a few bosons per lattice site, the total dimension of that space grows exponentially with the number of Bloch bands $\mathcal{N}$ used. The TDV approach reduces that dimension dramatically, potentially leading to a great improvement of the efficiency. Below, we will compare both approaches on a simple model system consisting of four lattice sites among which a total number of six bosons has been distributed. We assume periodic boundary conditions. On-site energies, hopping integrals, and interaction energies are calculated using Wannier functions for this four-site lattice.

Typically, we consider the first three to five bands for the MBH model. For the TDV simulation of this system, we consider a sufficient number of Bloch bands $\mathcal{N}_V$ to allow for convergence of the variational Wannier functions as this increases the total computational cost very little (usually convergence is reached for three to five bands).

The energy is measured in units of recoil energy $E_r = h^2/2m(2a)^2$ with $a = \lambda/2$ being the lattice constant. The depth of the lattice is typically set by us to $s = 10E_r$. Simulations of the TDV model are performed with *Mathematica*'s NDSOLVE function.

A. Ground state

The energy of a ground state can be used as a simple quantity enabling one to compare the accuracy of state representation over various variational manifolds. It has been calculated numerically for different coupling constant g's using up to five Bloch bands in both approaches. For the special case of a single Bloch band $\mathcal{N} = 1$, both methods obviously reduce to the same standard BH model and lead to the same ground-state energy. It is no longer true when more bands are taken into consideration. Let us denote $\mathcal{N}_M$ as the number of bands used within the MBH (keeping $\mathcal{N}_V$ for the variational approach).

In Fig. 1, estimates for the ground-state energy are presented. Notice that the TDV ansatz quickly leads to the apparent convergence of the estimated ground-state energy (for $\mathcal{N}_V \geqslant 3$), even for large values of the interaction constant. Observe also that, already, $\mathcal{N}_M = 2$ is sufficient in the MBH approach to yield lower estimates for the energy. Here for large g, a slow convergence with increasing $\mathcal{N}_M$ is observed. On the other hand, for small $g < 1$, TDV as well as MBH predictions become close to the standard BH model pointing out its region of validity.

The failure of TDV for larger g indicates that even the ground state in the model involves significant entanglement between particles, a feature absent in the variational ansatz (11) where all the particles at a given site are in the same variationally chosen Wannier state.

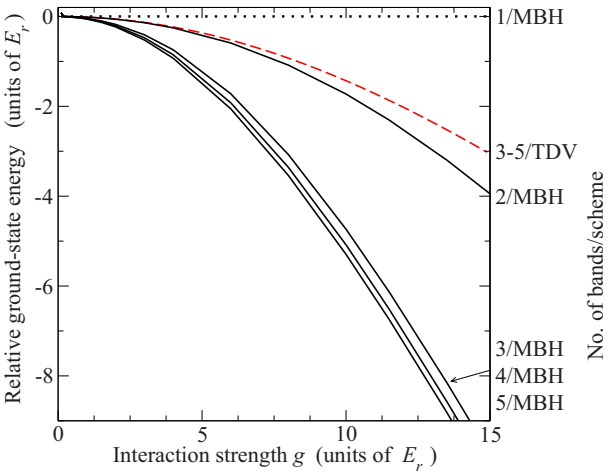

FIG. 1. (Color online) Ground-state energy for six particles in a four-site system with periodic boundary conditions calculated within the MBH model for $\mathcal{N}_M = 1$–5 Bloch bands included (black curves with number of bands indicated). Results for the variational ansatz of Ref. [28] are shown as a dashed red curve—they converge for $\mathcal{N}_V > 2$. The energy is shown with respect to the ground-state energy of the standard Bose-Hubbard model as a function of the coupling constant g. Clearly, for $g > 1$, the TDV approach based on (11) fails to approximate the ground-state energy.

B. Time evolution

Let us now compare time evolution in both approaches. Rather than starting this evolution from the appropriate ground states (which may differ significantly—see above), we consider model initial states that enlighten the differences between MBH and TDV results. The time evolution in the TDV model is performed by numerically solving the system of differential equations (18). For the MBH, a many-body Schrödinger equation is solved (which is easy for our small model cases).

We study evolution of the system using both approaches in three cases: with constant interaction strength but inhomogeneous distribution of bosons over sites, with a linearly quenched coupling constant, and with an oscillating one. Time-dependent g may be realized by varying the magnetic field $B(t)$ close to the Feshbach resonance. The alternative would be to vary the lattice depth s. That, for rapid changes in $s(t)$, may lead to additional effects [36], which, for clarity, we presently want to avoid.

1. *The inhomogeneous distribution of particles*

We numerically performed the evolution of the system with the initial state being a Fock state, containing the initial distribution of six particles over four lattice sites as (2,2,1,1). Particles in sites 1, 3, and 4 initially are confined to the lowest Bloch band, whereas, two particles localized in site 2 either also are set in the lowest Bloch band or are set in the first (second) excited band. During the numerical integration of the

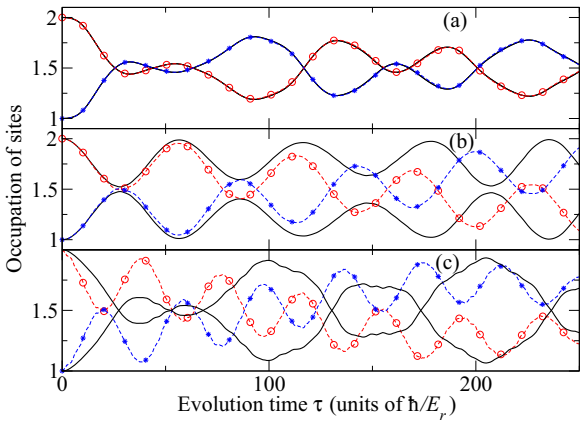

FIG. 2. (Color online) Population of lattice sites in time for the initial Fock state $|2,2,1,1\rangle$ (all particles in the lowest band) for different interaction strengths: panel (a) $g = 0.2$, panel (b) $g = 2$, and panel (c) $g = 4$. Results from the TDV approach are represented by black solid curves; MBH predictions are shown as colored curves with stars and circles. The first two and second two sites are equivalent due to assumed periodic boundary conditions.

time-dependent Schrödinger equation, populations of all four lattice sites are monitored.

Let us consider first the case when all the particles were set in the lowest Bloch band. If the interaction strength coupling constant g is small enough ($g \approx 0.2$), results obtained using both methods are virtually the same (compare Fig. 2). Due to the symmetry of the system, two sites having initially single occupancy are equivalent (the same holds for initially doubly occupied sites). Thus, only two distinct curves appear in the plot with population between sites being transferred in an oscillatory manner. For larger g, the predictions of both approaches start to diverge for longer times but for short enough times, remain similar, and TDV can be used in this regime to get approximate results (e.g., for $g = 1$ for the time of one oscillation). But when g is large, results for both methods differ considerably in a time shorter than a single oscillation (as for $g = 4$). All the results presented are obtained using three Bloch bands in the MBH. For the TDV method, we use up to five bands (we checked that the results are converged with respect to the number of bands in both approaches).

If the two particles are set in the first excited state in site 2, initially, the differences become much more striking (see Fig. 3). The variational approach is incapable of showing any transport of particles that occupied the first excited band into the adjacent sites. This is obviously incorrect and results from the restriction of the TDV ansatz in which all particles at a given site occupy the same time-dependent Wannier orbital. The MBH approach has no such a restriction.

In the case of particles set in the second excited state when interactions are set to zero, tunneling in the TDV model also does not appear. Only in the presence of interactions is some transport between sites restored, but obviously, it has a different interaction-based origin. In effect, the simulations in the MBH and TDV approaches show different results.

The difference between the TDV and the MBH results can be understood using a simplified case of two particles in a two-well system. Assume that, initially, the time-dependent Wannier function in the first site is purely a ground state ($w_1 = w_1^1$), whereas, in the second site, it is in an excited state ($w_2 = w_2^\epsilon$). The tunnelings between such Wannier states vanish $J_{12} = J_{21} = 0$. The transport between sites may result from interactions only provided that the bands are of the same symmetry. For the opposite symmetry of bands, the parity rule discussed in the context of Eq. (20) implies vanishing coupling between sites. Then $i\dot{C}_{\vec{n}}(t) = \langle\vec{n}|H_V(t)|\vec{n}\rangle C_{\vec{n}}(t)$ only gives a phase change, and occupations remain constant.

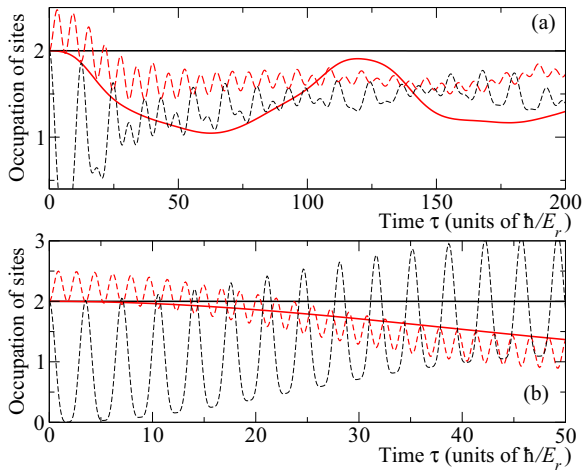

FIG. 3. (Color online) Populations of different lattice sites in time for [panel (a)] the initial Fock state $|2^+,2,1,1\rangle$ and [panel (b)] $|2^{++},2,1,1\rangle$, where "+" ("++") denote occupation by both particles of the first (second) excited Bloch band. Black curves show the occupation of site 1, and red curves show the occupation of site 2. Solid (dashed) lines represent results obtained with the help of TDV (MBH) models. The site in which particles originally resided in the excited band is not depleted at all within the TDV approach if the excited band has opposite parity (the case shown in the top plot with $g = 0.2$) or if the atoms are noninteracting (bottom plot, $g = 0$).

2. *Quench*

Consider a simple quench scenario, a linear change in the strength of two-particle interactions from initial value g_{ini} to g_{fin} over time τ. The initial state has been prepared in the ground state of the single-band BH model with $g = g_{\text{ini}}$. This assures the same initial state for both methods. Numerical solution of the time-dependent Schrödinger equation is performed by means of a Runge-Kutta numerical scheme, both for the MBH model and for the TDV approach. Figure 4 illustrates two cases: $(g_{\text{ini}}, g_{\text{fin}}) = (0.2, 1)$ and $(g_{\text{ini}}, g_{\text{fin}}) = (1, 5)$. For a sufficiently slow quench, the final energy of the system after the quench is close to the ground-state energy of the Hamiltonian with $g = g_{\text{fin}}$. Note that we have started from a good approximation of the ground state for small initial $g = g_{\text{ini}}$ but not exactly from a ground state, so we do not expect to reach the ground state at the end of the quench even in the $\tau \to \infty$ limit. Obviously, however, these final ground-state energies give the lower bound for the energies possible to obtain using both methods. From Fig. 4, it is clear that, indeed, the difference between predictions for the final

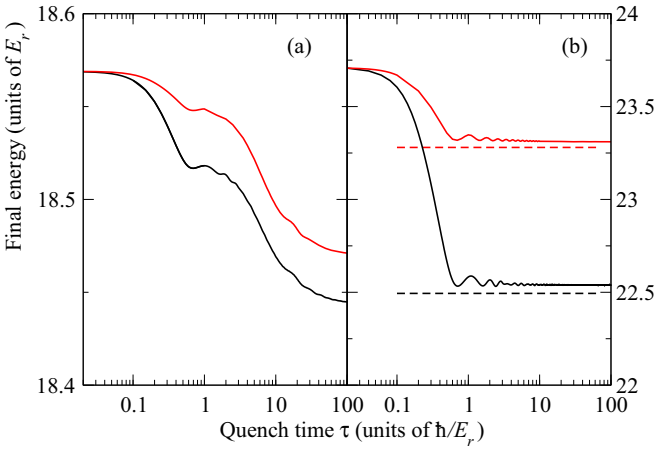

FIG. 4. (Color online) Final energy after a linear quench of interaction strength g during time τ, in panel (a), starting from $g_{\text{ini}} = 0.2$ up to $g_{\text{fin}} = 1.0$ and in panel (b), $g_{\text{ini}} = 1.0$, $g_{\text{fin}} = 5.0$. Red (upper) solid curves show results obtained using the TDV method (for five bands), whereas, black thicker lines correspond to the simulation using the MBH model (with three bands). Horizontal dashed lines show ground-state energies for corresponding methods (see text).

energy is largely due to the inability of the TDV ansatz to reproduce the ground-state energy accurately for large values of g.

One may observe, however, that the excess energy over the corresponding ground state as well as the shape of the energy versus quench time dependence is quite similar in both MBH and TDV approaches.

3. *Modulation*

Periodic modulations of system parameters (e.g., optical lattice depth or the interaction strength) serves as a mean to transfer the energy to cold atomic systems. Sensitivity of the process with respect to the modulation frequency allows for finding excitation spectra providing, e.g., information about the energy gap in the system [7,37] or enabling studying the multiband interaction effects [38]. Larger modulation frequencies help to control effective tunnelings [39], and resonant driving may lead to a direct population of excited bands [36,40]. Analysis of periodic modulations also has been a useful theoretical-numerical tool [41] for access to the exited states of BH-like systems.

Here we consider a periodic modulation of the system by varying the interaction coupling constant: $g(t) = g_0 + g_{\mathrm{mod}} \sin \omega t$. Specifically, we take $g_0 = 1$, $g_{\mathrm{mod}} = 0.1$. The depth of the lattice potential is assumed to be $s = 25E_r$, deep in the Mott regime with vanishing tunneling. Then the analysis may be reduced to a single site in which we put two particles. The initial state is a single Bloch-band ground state. This initial condition has an overlap over 98% on the energy minimum state in the variational manifold and a similar value on the MBH ground state. At characteristic resonant frequencies, one expects that strong Rabi oscillations occur manifesting efficient excitation of excited bands. To detect the resonance, it is sufficient to measure the depletion of the initial state. In parallel to Ref. [40], we define a transfer efficiency function,

$$D(\omega) = 1 - \inf_{t\in[0,T]} |\langle\psi(0)|\psi(t)\rangle|, \tag{21}$$

where T is a fixed (long) evolution time.

The depletion as a function of the frequency of modulation is shown in Fig. 5. The MBH shows two prominent peaks at $\omega \approx 15.9E_r$ and $\omega \approx 17.5E_r$. The latter may be identified as a double occupancy of the first excited Bloch band. This is strictly forbidden in the TDV model: As mentioned before, occupation of Bloch bands 2,4,6, ..., when starting from the initial state containing particles populating 1,3,5, ... bands (in our case, only the first band), is not possible. Thus, the corresponding peak in the TDV approach is missing.

Another noteworthy feature of Fig. 5 is a noticeable, although small, shift in the single (in this frequency range) absorption peak in the TDV case. This peak is identified in the MBH model as the interaction-induced promotion of two particles to the second excited Bloch band. The TDV dynamics shows a similar behavior with significant population of the second excited band. The striking asymmetry of the TDV peak (compare Fig. 5) with a sharp drop (be aware of the mirror image) on the right-hand side is an unexplained peculiarity of TDV approach numerics. This is not a numerical instability as checked by high-precision arithmetics using the *Mathematica* code.

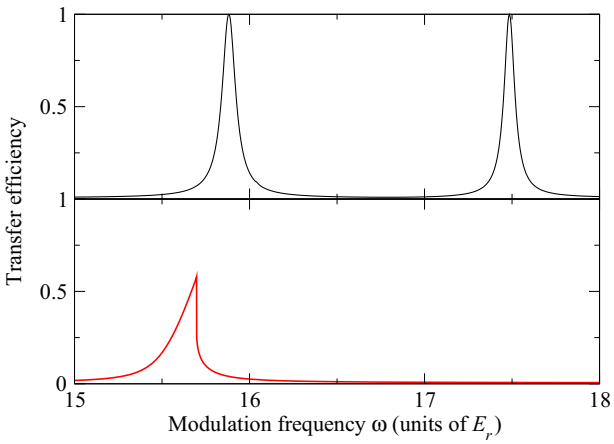

FIG. 5. (Color online) Transfer efficiency from the ground state during a modulation of total duration $T = 400\hbar/E_r$. The top panel shows the MBH results, and the lower panel (in the mirror image) corresponds to the TDV model calculations.

The state in which two particles occupy the same site: One in the lowest Bloch band, the other in the second excited band is as follows: $\psi_{13} = \hat{b}_k^{1\dagger}\hat{b}_k^{3\dagger}|\Omega\rangle$ is not representable by the variational ansatz. Indeed, such a state is a maximally entangled state of two particles. The maximal overlap of ψ_{13} over a variational product state: $|\langle\psi_{13}|\frac{1}{\sqrt{2}}(\alpha b_k^{1\dagger} + \beta b_k^{3\dagger})^2|\Omega\rangle|$, $|\alpha|^2 + |\beta|^2 = 1$ is $\frac{1}{\sqrt{2}}$ and is reached when $\alpha = \beta = \frac{1}{\sqrt{2}}$. Such a state has an energy of $E_1 + E_3$ just as state ψ_{13}. This is quite accurately represented in the simulations: The position of the MBH peak is $15.9E_r$, whereas, the TDV model leads to a highly asymmetric peak situated at $15.7E_r$. Presumably, this shape reflects the drawback of the oversimplified variational space used by the ansatz (11).

V. GENERALIZATION OF THE TDV METHOD

The variational approach fails in the situations described in this paper, largely due to a large truncation of the Hilbert space, a truncation denying any possibility for the on-site entanglement to be present in the system. This may be, to some extent, improved by introducing more variational bands in the TDV model, leading, however, to a further complication of the model. Hopefully, in some cases, the number of bands may be kept rather small, allowing for a reasonable computational efficiency. For example, for modulation spectroscopy, allowing for just one additional variational band would include state $a_1^\dagger a_3^\dagger|\Omega\rangle$, coupled by a resonance to the ground state in the variational space. Excitations of these type dominate modulation spectra [27,42,43].

Let us describe the proposed extension of the TDV method in some detail. In the complete analogy to the single variational band approach, we suggest defining $D > 1$ variational bands (here we consider $D = 2$). Equation (11) is generalized to

$$w_k^\kappa(x,t) = \sum_{\alpha=1}^{\mathcal{N}_V} d_k^{\alpha,\kappa}(t) w_k^{\alpha,\kappa}(x) \quad \text{for} \quad \kappa = 1,\ldots,D. \tag{22}$$

The orthonormality is imposed: $\langle w_k^{\kappa}(x,t), w_k^{\kappa'}(x,t)\rangle = \delta_{\kappa,\kappa'}$. To obtain equations for the time evolution, the time-dependent variational principle could be used again.

Here we test the effect of including D variational bands instead of just one by comparing the ground-state energy computation. The energy functional being minimized reads

$$\hat{H} = \sum_{k=1}^{L}\Bigg[\sum_{\kappa,\lambda,\mu,\nu=1}^{D}\frac{1}{2}U_k^{(\kappa,\lambda,\mu,\nu)}(t)b_k^{(\kappa)\dagger}(t)b_k^{(\lambda)\dagger}(t)b_k^{(\mu)}(t)b_k^{(\nu)}(t) + \sum_{\mu,\nu=1}^{D}\Big(E_k^{(\mu,\nu)}(t)b_k^{(\mu)\dagger}(t)b_k^{(\nu)}(t) - J_{k,k+1}^{(\mu,\nu)}(t)b_k^{\dagger(\mu)}(t)b_{k+1}^{(\nu)}(t) + \text{c.c.}\Big)\Bigg], \tag{23}$$

where

$$E_k^{(\mu,\nu)}(t) = \int w_k^{\mu *}(x,t)\hat{h}(t)w_k^{\nu}(x,t)dx,$$
$$J_{k,k+1}^{(\mu,\nu)}(t) = \int w_k^{\mu *}\hat{h}(t)w_{k+1}^{\nu}(x,t)dx, \tag{24}$$
$$U_{kkkk}^{(\kappa,\lambda,\mu,\nu)}(t) = \int w_k^{\kappa *}(x,t)w_k^{\lambda *}(x,t)w_k^{\mu}(x,t)w_k^{\nu}(x,t)dx,$$

we cannot omit one-particle cross terms (for example, $E_k^{(1,2)}$) because generalized Wannier functions for different variational bands are not formed by eigenstates confined to a single Bloch band. Such a TDV model with $D = 2$ is compared with the MBH model in Fig. 6. For $D < \mathcal{N}_V < \mathcal{N}_M$, the TDV space is smaller than the Hilbert space of the MBH model. If, however, $D < \mathcal{N}_M < \mathcal{N}_V$, it is not obvious which approach should be more efficient. The complexity of calculations within the limits of the ansatz given by Eq. (22) depends largely on D, not on $\mathcal{N}_V$, thus, the $D < \mathcal{N}_M < \mathcal{N}_V$ situation is the only one that

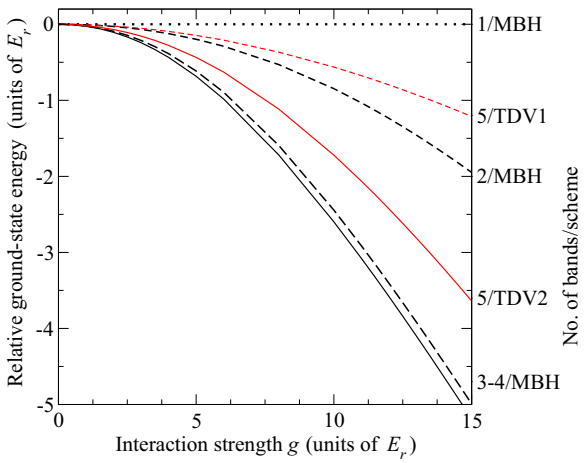

FIG. 6. (Color online) Ground-state energy for four particles distributed on three sites calculated within the MBH model for $\mathcal{N}_M = 1,\ldots,4$ Bloch bands included (black curves). Results for the variational ansatz with $D = 1,2$ and $\mathcal{N}_V = 5$ are shown in red. The energy is presented with respect to the ground-state energy of the standard BH model.

may result in the variational method boosting the efficiency of the computation.

Exemplary application of the TDV ansatz for $D = 2$ is presented in Fig. 6 for four particles residing on the three-site system. We have found that $D = 2$ leads to a significant improvement in the estimate for the ground-state energy as compared to the $D = 1$ proposition [28]. In both calculations, $\mathcal{N}_V = 5$. Disappointingly, however, a comparison with the MBH model shows that a full three-band calculation is superior to the TDV ansatz with $D = 2$. Thus, although the latter constitutes a significant improvement over the $D = 1$ case, it still does not catch the complexity involved in the ground state of the system, in particular, for higher interaction strength g values. Seemingly, multiparticle entanglement (missing for $D = 2$ that captures two-particle entanglement only) becomes important.

It would be desirable to also compare $D = 1$ and $D = 2$ results of the TDV approach for a slightly larger system of six particles on four sites as previously discussed for $D = 1$. Unfortunately, for $D = 2$, the TDV procedure seems to be quite ineffective, leading to a significant slow down of the minimization procedure due to a large number of local energy minima in a highly nonlinear variational equation. This casts a shadow on a possible application of the TDV approach for really interesting cases.

VI. CONCLUSIONS

For the system of interacting bosons in an optical lattice, we have performed extensive comparisons of two different methods, namely, the time-dependent variational approach (as proposed in Ref. [28]) and the multiband Bose-Hubbard expansion. Unfortunately, we have found that the TDV approach, while computationally less demanding, provides little alternatives for moderate and strong interatomic interactions and nontrivial time dependence of the system. Even extending the TDV approach to a richer Hilbert space taking two-particle entangled states into account only helps a little. For the ground-state energy estimation, the gain resulting from using two variational bands is smaller than that obtained from three standard single-particle bands. That shows that the genuine ground state of strongly interacting bosons in optical lattices constitutes a clear example of multiparticle entanglement. Further increasing the number of variations seems not practical due to the enhanced complexity of the approach and the growth of the on-site Hilbert-space dimension.

Both interaction strength quenches and its modulation may lead to significant excitation of entangled modes—in such cases, the TDV approach clearly fails to capture the details of the physics involved. Moreover, for periodic modulation of the interaction strength, we have observed strange asymmetry in modulation spectra in the TDV approach, probably reflecting the fact that the variational space is strongly restricted. Although the modulation spectra asymmetry would disappear enlarging the variational space taking two variational bands per site, as for the ground-state calculations, the increased complexity of the approach would not compensate for its drawbacks, clearly shown for the ground state above.

ACKNOWLEDGMENTS

J.M. and J.Z. acknowledge support of the Polish National Science Centre Grant No. DEC-2012/04/A/ST2/00088. M.Ł. acknowledges support from the Polish National Science Center by means of Project No. 2013/08/T/ST2/00112 for a Ph.D. thesis and Research Grant No. DEC-2011/01/N/ST2/02549 from the same institution. M.Ł. also acknowledges a special stipend of the Smoluchowski Scientific Consortium "Matter Energy Future." Simulations were carried out at ACK Cyfronet AGH, part of PL-Grid project and on the Deszno supercomputer (IF UJ) obtained in the framework of the Polish Innovation Economy Operational Program (Grant No. POIG.02.01.00-12-023/08).

[1] M. Lewenstein, A. Sanpera, V. Ahufinger, B. Damski, A. Sen, and U. Sen, Adv. Phys. **56**, 243 (2007).

[2] M. Lewenstein, A. Sanpera, and V. Ahufinger, *Ultracold Atoms in Optical Lattices: Simulating Quantum Many-Body Systems* (Oxford University Press, Oxford, 2012).

[3] H. A. Gersch and G. C. Knollman, Phys. Rev. **129**, 959 (1963).

[4] D. Jaksch, C. Bruder, J. I. Cirac, C. W. Gardiner, and P. Zoller, Phys. Rev. Lett. **81**, 3108 (1998).

[5] P. Jessen and I. Deutsch, Adv. At., Mol., Opt. Phys. **37**, 95 (1996).

[6] C. Becker, P. Soltan-Panahi, J. Kronjäger, S. Dörscher, K. Bongs, and K. Sengstock, New J. Phys. **12**, 065025 (2010).

[7] T. Stöferle, H. Moritz, C. Schori, M. Köhl, and T. Esslinger, Phys. Rev. Lett. **92**, 130403 (2004).

[8] T. D. Kühner and H. Monien, Phys. Rev. B **58**, R14741 (1998).

[9] T. Giamarchi, *Quantum Physics in One Dimension*, International Series of Monographs on Physics (Oxford University Press, Oxford, 2004).

[10] M. P. A. Fisher, P. B. Weichman, G. Grinstein, and D. S. Fisher, Phys. Rev. B **40**, 546 (1989).

[11] W. Kohn, Phys. Rev. **115**, 809 (1959).

[12] S. Kivelson, Phys. Rev. B **26**, 4269 (1982).

[13] D. van Oosten, P. van der Straten, and H. T. C. Stoof, Phys. Rev. A **67**, 033606 (2003).

[14] R. B. Diener and T.-L. Ho, Phys. Rev. Lett. **96**, 010402 (2006).

[15] A. Koetsier, D. B. M. Dickerscheid, and H. T. C. Stoof, Phys. Rev. A **74**, 033621 (2006).

[16] P. O. Fedichev, M. J. Bijlsma, and P. Zoller, Phys. Rev. Lett. **92**, 080401 (2004).

[17] D. B. M. Dickerscheid, U. Al Khawaja, D. van Oosten, and H. T. C. Stoof, Phys. Rev. A **71**, 043604 (2005).

[18] M. Wouters and G. Orso, Phys. Rev. A **73**, 012707 (2006).

[19] H. P. Büchler, Phys. Rev. Lett. **104**, 090402 (2010).

[20] X. Cui, Y. Wang, and F. Zhou, Phys. Rev. Lett. **104**, 153201 (2010).

[21] J. von Stecher, V. Gurarie, L. Radzihovsky, and A. M. Rey, Phys. Rev. Lett. **106**, 235301 (2011).

[22] U. Schollwoeck, Ann. Phys. (NY) **326**, 96 (2011).

[23] P. R. Johnson, E. Tiesinga, J. V. Porto, and C. J. Williams, New J. Phys. **11**, 093022 (2009).

[24] A. Mering and M. Fleischhauer, Phys. Rev. A **83**, 063630 (2011).

[25] U. Bissbort, F. Deuretzbacher, and W. Hofstetter, Phys. Rev. A **86**, 023617 (2012).

[26] D.-S. Lühmann, O. Jürgensen, and K. Sengstock, New J. Phys. **14**, 033021 (2012).

[27] M. Łącki, D. Delande, and J. Zakrzewski, New J. Phys. **15**, 013062 (2013).

[28] K. Sakmann, A. I. Streltsov, O. E. Alon, and L. S. Cederbaum, New J. Phys. **13**, 043003 (2011).

[29] D. Jaksch, V. Venturi, J. I. Cirac, C. J. Williams, and P. Zoller, Phys. Rev. Lett. **89**, 040402 (2002).

[30] S. Albeverio, F. Gesztezy, R. Høegh-Krohn, and H. Holden, *Solvable Models in Quantum Mechanics*, 2nd ed., AMS Chelsea Publishing Series (AMS, Providence, 2005).

[31] O. Dutta, A. Eckardt, P. Hauke, B. Malomed, and M. Lewenstein, New J. Phys. **13**, 023019 (2011).

[32] P. A. M. Dirac, Math. Proc. Cambridge Philos. Soc. **26**, 361 (1930).

[33] J. Frenkel, *Wave Mechanics, Advanced General Theory* (Clarendon, Oxford, 1934).

[34] A. McLachlan, Mol. Phys. **8**, 39 (1964).

[35] J. Broeckhove, L. Lathouwers, E. Kesteloot, and P. Van Leuven, Chem. Phys. Lett. **149**, 547 (1988).

[36] M. Łącki and J. Zakrzewski, Phys. Rev. Lett. **110**, 065301 (2013).

[37] A. Iucci, M. A. Cazalilla, A. F. Ho, and T. Giamarchi, Phys. Rev. A **73**, 041608 (2006).

[38] M. J. Mark, E. Haller, K. Lauber, J. G. Danzl, A. J. Daley, and H.-C. Nägerl, Phys. Rev. Lett. **107**, 175301 (2011).

[39] A. Eckardt, C. Weiss, and M. Holthaus, Phys. Rev. Lett. **95**, 260404 (2005).

[40] T. Sowiński, Phys. Rev. Lett. **108**, 165301 (2012).

[41] J. Zakrzewski and D. Delande, Phys. Rev. A **80**, 013602 (2009).

[42] M. Łącki, D. Delande, and J. Zakrzewski, Phys. Rev. A **86**, 013602 (2012).

[43] J.-W. Huo, F.-C. Zhang, W. Chen, M. Troyer, and U. Schollwöck, Phys. Rev. A **84**, 043608 (2011).